

1 Supporting Information for  
2 **High secondary formation of nitrogen-containing organics (NOCs) and its possible**  
3 **link to oxidized organics and ammonium**

4

5 Guohua Zhang<sup>1</sup>, Xiufeng Lian<sup>1,2</sup>, Yuzhen Fu<sup>1,2</sup>, Qin hao Lin<sup>1</sup>, Lei Li<sup>3</sup>, Wei Song<sup>1</sup>, Zhanyong Wang<sup>4</sup>,  
6 Mingjin Tang<sup>1</sup>, Duohong Chen<sup>5</sup>, Xinhui Bi<sup>1,\*</sup>, Xinming Wang<sup>1</sup>, Guoying Sheng<sup>1</sup>

7

8 <sup>1</sup> State Key Laboratory of Organic Geochemistry and Guangdong Key Laboratory of Environmental  
9 Resources Utilization and Protection, Guangzhou Institute of Geochemistry, Chinese Academy of  
10 Sciences, Guangzhou 510640, PR China

11 <sup>2</sup> University of Chinese Academy of Sciences, Beijing 100039, PR China

12 <sup>3</sup> Institute of Mass Spectrometer and Atmospheric Environment, Jinan University, Guangzhou 510632,  
13 China

14 <sup>4</sup> School of Intelligent Systems Engineering, Sun Yat-sen University, Shenzhen 518107, PR China

15 <sup>5</sup> State Environmental Protection Key Laboratory of Regional Air Quality Monitoring, Guangdong  
16 Environmental Monitoring Center, Guangzhou 510308, PR China

17

## 18 **Instrumentation**

19 Individual particles are introduced into SPAMS through a critical orifice. They are  
20 focused and accelerated to specific velocities, which are determined by two continuous  
21 diode Nd:YAG laser beams (532 nm). Based on the measured velocities, a pulsed laser  
22 (266 nm) downstream is triggered to desorb/ionize the particles. The produced positive and  
23 negative molecular fragments are recorded. In summary, a velocity, a detection moment,  
24 and an ion mass spectrum are recorded for each ionized particle, while there is no mass  
25 spectrum for not ionized particles. The velocity could be converted to  $d_{va}$  based on a  
26 calibration using polystyrene latex spheres (PSL, Duke Scientific Corp., Palo Alto) with  
27 predefined sizes.

28 The concentrations of  $\text{NO}_x$ , and  $\text{O}_3$  were measured by Model 42i (NO- $\text{NO}_2$ - $\text{NO}_x$ )  
29 Analyzer, and Model 49i  $\text{O}_3$  Analyzer (Thermo Fisher Scientific Inc.), respectively. The  
30 concentrations of  $\text{PM}_{2.5}$  were continuously measured using a tapered element oscillating  
31 microbalance (TEOM 1405, Thermo Fisher Scientific Inc.), respectively.

32

## 33 **Positive matrix factorization analysis**

34 PMF is a multivariate receptor model used to determine source factors, and it has  
35 been used extensively with temporal variation data. In order to complement single  
36 particle data analysis, we used USEPA PMF 5.0 (Norris et al., 2009) to group chemical  
37 markers from all the detected particles. In such analysis, RPAs for ion markers were  
38 typically used as input in the PMF model. For this study, an uncertainty of 50% in RPA  
39 was used due to the shot-to-shot fluctuations of desorption laser and complex particle

40 matrix (Zauscher et al., 2013). 14 marker ions with were used, including sulfate (-  
41 97[HSO<sub>4</sub>]<sup>-</sup>), nitrate (-62[NO<sub>3</sub>]<sup>-</sup>), ammonium (18[NH<sub>4</sub>]<sup>+</sup>), oxalate (89[HC<sub>2</sub>O<sub>4</sub>]<sup>-</sup>), oxidized  
42 organics markers (at m/z -45[HCO<sub>2</sub>]<sup>-</sup>, m/z -59[CH<sub>3</sub>CO<sub>2</sub>]<sup>-</sup>, m/z -71[C<sub>3</sub>H<sub>3</sub>O<sub>2</sub>]<sup>-</sup>, m/z -  
43 73[C<sub>2</sub>HO<sub>3</sub>]<sup>-</sup>, m/z -87[C<sub>3</sub>H<sub>3</sub>O<sub>3</sub>]<sup>-</sup>, m/z -103[C<sub>3</sub>H<sub>3</sub>O<sub>4</sub>]<sup>-</sup>, and m/z -117[C<sub>4</sub>H<sub>5</sub>O<sub>4</sub>]<sup>-</sup>), organic  
44 nitrogen markers (NOCs, sum of -42[CNO]<sup>-</sup> and -26[CN]<sup>-</sup>), and other carbonaceous  
45 fragments (i.e., 36[C<sub>3</sub>]<sup>+</sup>, 37[C<sub>3</sub>H]<sup>+</sup>).

46 PMF solutions with 2–5 factors were tested, and the relevant Q values and Q<sub>robust</sub> /  
47 Q<sub>theory</sub> for these solutions are shown in Table S3. In these solutions explored Q<sub>robust</sub> /  
48 Q<sub>theory</sub> < 1, although it is recommended that Q<sub>robust</sub> ≈ Q<sub>theory</sub>. The 3-factor solution was  
49 chosen as the best because the measured versus predicted RPA of more relevant chemical  
50 species (i.e., NOCs, the oxidized organics and ammonium) in the PMF model had strong  
51 correlations (R<sup>2</sup> = 0.56–0.95), and also has the most physically meaningful factors. The  
52 residuals of this solution were between -2 and 2. In the 4 and 5-factor solution, with  
53 slightly stronger R<sup>2</sup> values than the 3-factor solution for NOCs and ammonium, but had  
54 two similar oxalate factors or an additional methylglyoxal factor, respectively, which  
55 seemed less physically meaningful. Bootstrapping on the 3-factor solution shows stable  
56 results, with > 90 out of 100 bootstrap factors mapped with those in the based run. F<sub>peak</sub>  
57 value from -0.5 to 0.5 was examined, and an examination of Q values showed the  
58 application of F<sub>peak</sub> of 0 giving the best result.

59

60 **Limited dependent of NOCs on the oxidized organics during spring and ammonium**  
61 **during summer**

62 During summer, the hourly detected number of NOCs showed a limited dependent on  
63 ammonium (Fig. 3d). As shown in Fig. S4, the detected number of ammonium is obviously  
64 lower than NOCs. In contrast, there were prevalent oxidized organics that were associated  
65 with NOCs. Due to the volatility of ammonium nitrate, there is less particulate ammonium  
66 in summer. Higher level of  $\text{NH}_3$  during summer (Pan et al., 2018) may have potential  
67 influence on the formation of NOCs. Less dependence of NOCs on ammonium could be  
68 due to the more predominant formation of secondary NOCs through the uptake of  $\text{NH}_3$  and  
69 the following interactions with secondary oxidized organics. As shown by Nguyen et al.  
70 (2012), ammonia is more efficient for the formation of NOCs in this pathway than  
71 ammonium. As also supported with PMF results shown in Fig. 5, the oxidized organics  
72 factor dominant contributed to the predicted NOCs during warmer seasons. Limited  
73 ammonium in this factor may indicate that abundance of oxidized organics during warmer  
74 season consumed the available ammonium. As discussed, such chemistry would even lead  
75 to a reduction in the concentrations of  $\text{NH}_3$  and  $\text{NH}_4^+$  through a model simulation (Zhu et  
76 al., 2018). However, NOCs showed a limited dependent on the oxidized organics during  
77 spring (Fig. 3a and 3b). Consistently, the lowest fraction of NOCs that contained the  
78 oxidized organics was observed (Fig. S4), and ammonium factor explained ~80% of the  
79 predicted NOCs (Fig. 5) during spring. It is likely attributed to the higher conversion of  
80 oxidized organics to the observed NOCs in humid air during spring (Fig. 6 and Table S1).  
81 In addition, possible reasons might also include more primary NOCs and unidentified  
82 oxidized organics.

83 Table S1. The number and Nfs of NOCs-containing particles in the all the detected  
 84 particles during four seasons, respectively. Standard errors for the Nfs of particles were  
 85 estimated assuming Poisson distribution(Pratt et al., 2010). Temperature (T), relative  
 86 humidity (RH), O<sub>3</sub>, and PM<sub>2.5</sub> were provided by Guangdong Environmental Monitoring  
 87 Center. The arriving air masses in Guangzhou, have been described previously: prevalence  
 88 of marine air masses in spring and summer, whereas northern air masses from inland China  
 89 in autumn and winter.

90

	Spring	Summer	Autumn	Winter
Num. of all the detected particles	933934	719371	1202604	397637
Nfs of NOCs-containing particles	58.7 ± 0.08%	59.4 ± 0.09%	59.0 ± 0.07%	55.6 ± 0.1%
Temperature (°C)	18.8 ± 4.2	29.0 ± 2.7	24.9 ± 2.6	11.3 ± 2.3
Relative Humidity (%)	68.0 ± 13.4	66.0 ± 11.4	47.0 ± 10.1	43.0 ± 19.1
O <sub>x</sub> (μg m <sup>-3</sup> )	100.4 ± 43.7	114.5 ± 70.6	136.3 ± 35.4	113.1 ± 34.0
PM <sub>2.5</sub> (μg m <sup>-3</sup> )	51.2 ± 26.0	31.9 ± 21.0	44.3 ± 18.1	55.3 ± 28.9

91

92 Table S2. Coefficients calculated with a multiple linear regression analysis of the  
93 RPAs of NOCs and those of the oxidized organics and ammonium. All the regressions  
94 show significant correlation, with the fitting coefficients shown with a standard error.  
95

	The oxidized organics	Ln (Ammonium)	R <sup>2</sup>
Spring	4.24 ± 0.36	-0.0064 ± 0.00057	0.24
Summer	1.69 ± 0.22	-0.012 ± 0.0013	0.24
Autumn	1.27 ± 0.09	-0.0086 ± 0.0011	0.38
Winter	1.57 ± 0.14	-0.0010 ± 0.00069	0.57
Autumn 2014	1.18 ± 0.11	-0.013 ± 0.0042	0.35

96

97 Table S3. Q values for PMF Analysis with different number of factors.

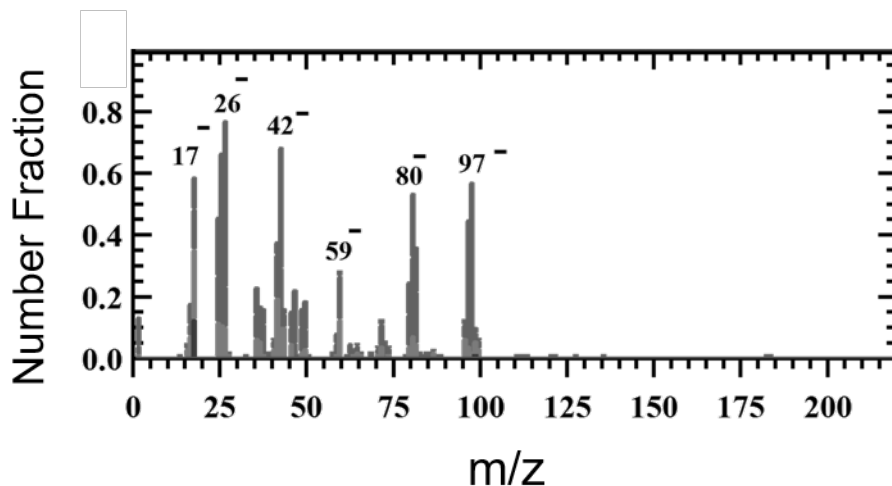
98

Num. of factors	R <sup>2#</sup> for all the input species	R <sup>2</sup> for NOCs	R <sup>2</sup> for the oxidized organics	R <sup>2</sup> for ammonium	Q <sub>robust</sub> *	Q <sub>robust</sub> / Q <sub>theory</sub>
2	0.28-0.95	0.28	0.44-0.95	0.46	12110	0.76
3	0.25-0.95	0.74	0.59-0.95	0.56	8278	0.59
4	0.49-0.92	0.78	0.59-0.92	0.64	6485	0.53
5	0.41-0.94	0.83	0.58-0.94	0.66	4944	0.47

99

100 # R<sup>2</sup> between the observed and predicted species

101 \* Q<sub>robust</sub> with F<sub>peak</sub> = 0.

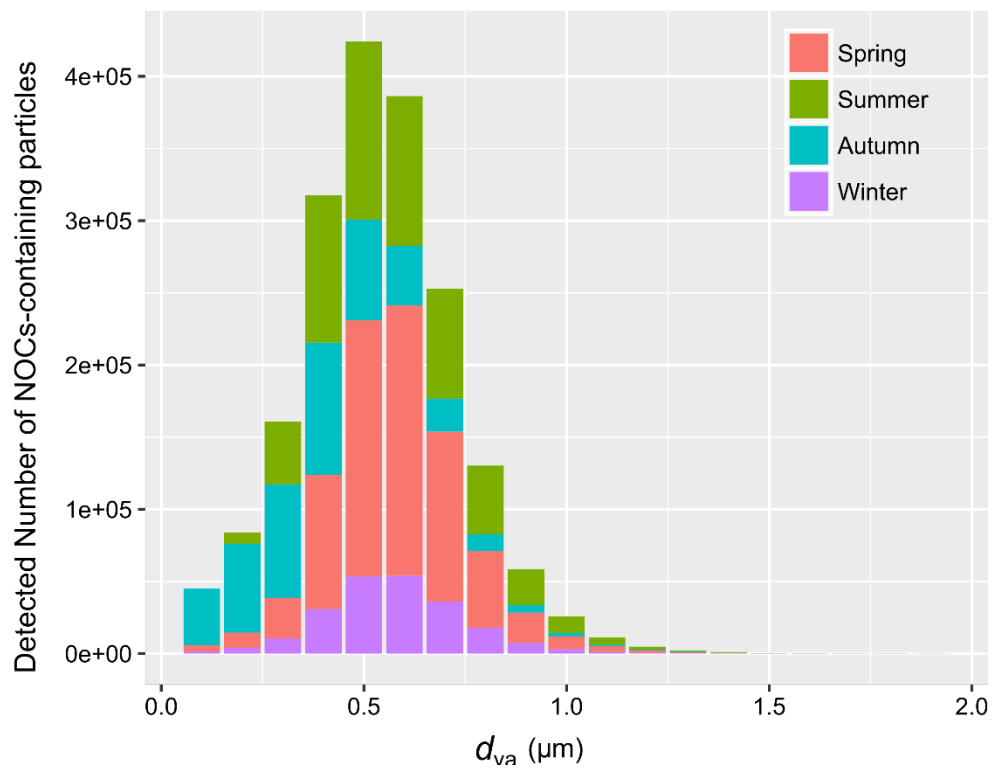


102

103

104 **Figure S1.** The number fraction of ion peaks versus m/z from the bulk solution-phase  
 105 reaction of ammonium sulfate and methylglyoxal. The bulk solution-phase reaction was  
 106 prepared with 1M ammonium sulfate and 1M methylglyoxal solution, and aged in sealed  
 107 bottles under dark conditions and at room temperature for several days. BrC SOA formed  
 108 from such reaction has been previously reported to be significantly contributed from  
 109 NOCs (Aiona et al., 2017).

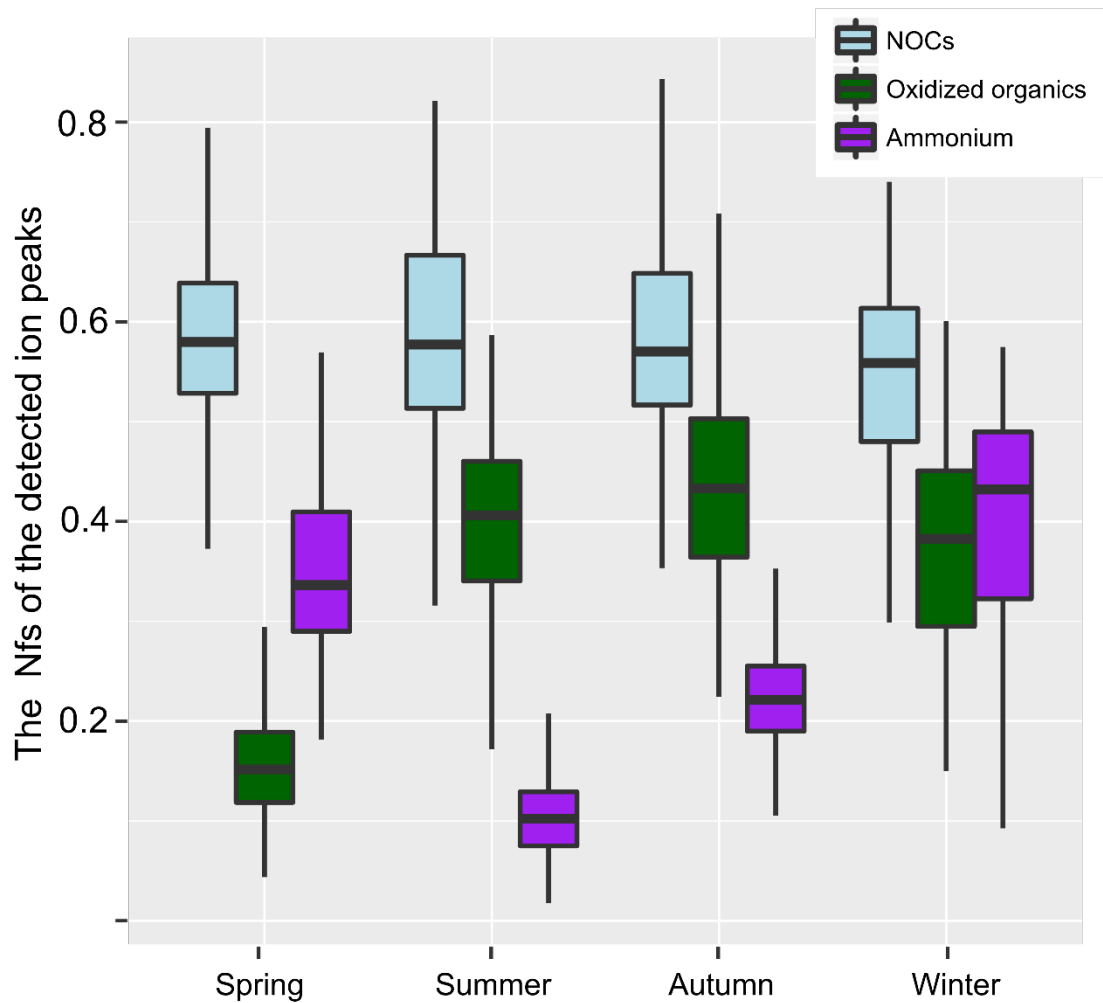




110

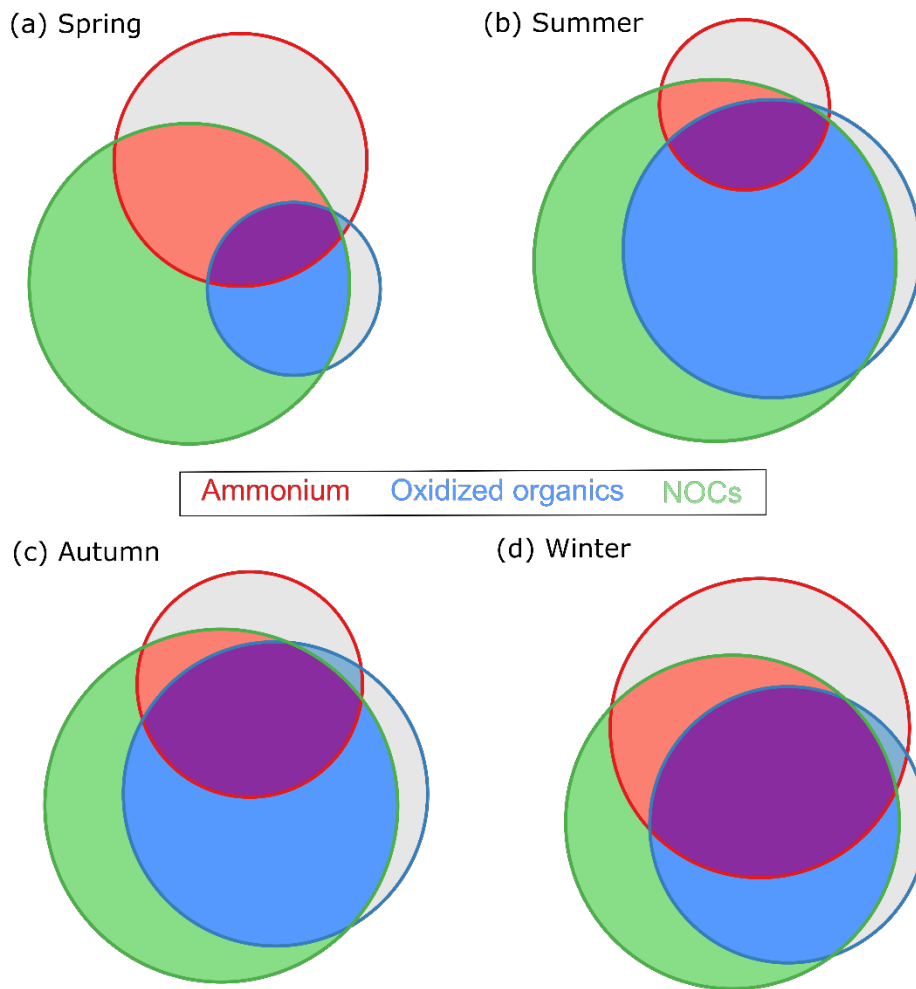
111

112 **Figure S2.** The detected number of NOC-containing particles along  $d_{va}$ .



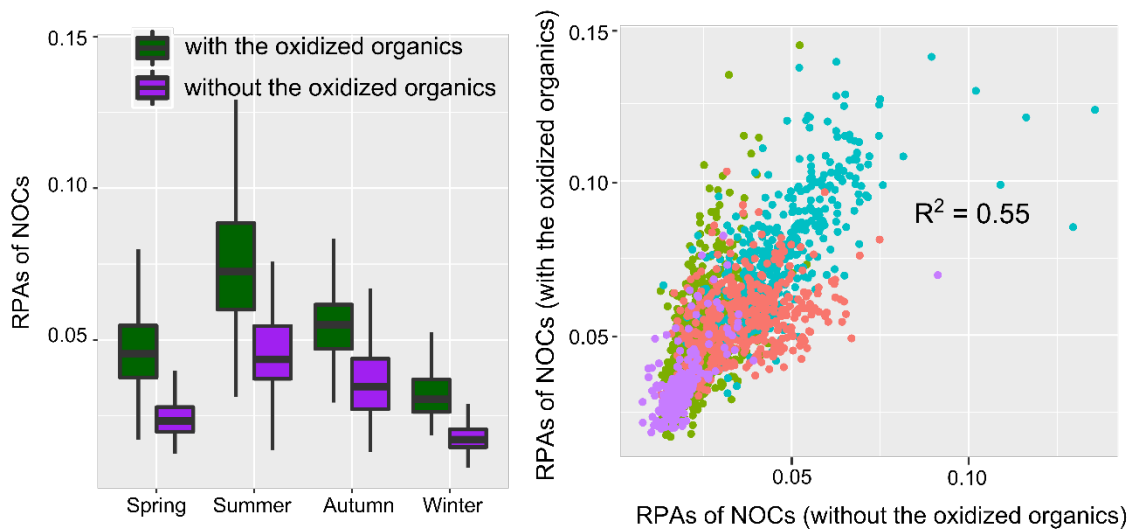
113  
114

115 **Figure S3.** The distribution of the Nfs of the detected ion peaks over four seasons.



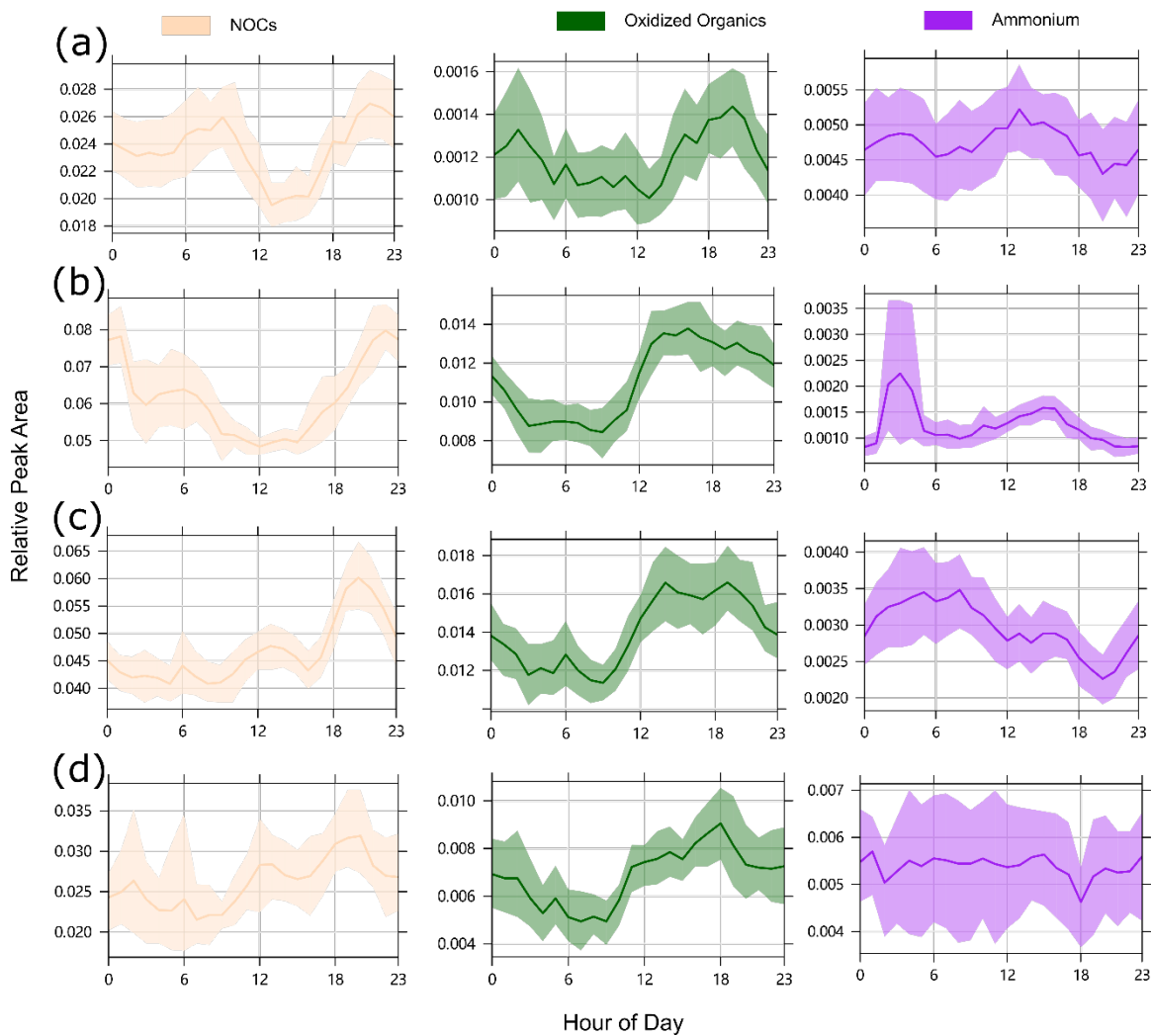
116  
117

118 Figure S4. Venn plot of number based mixing state involving NOCs (green circle), the  
119 oxidized organics (blue circle), and ammonium (red circle).



120  
121

122 Figure S5. (left) Comparison and (right) correlation analysis of RPAs of NOCs in NOCs-  
 123 containing particles internally/externally mixed with the oxidized organics. The NOCs-  
 124 containing particles externally mixed with the oxidized organics is expected to containing  
 125 relatively lower abundance of NOCs, as pre-existing limited oxidized organics were  
 126 likely totally consumed in the formation of NOCs.

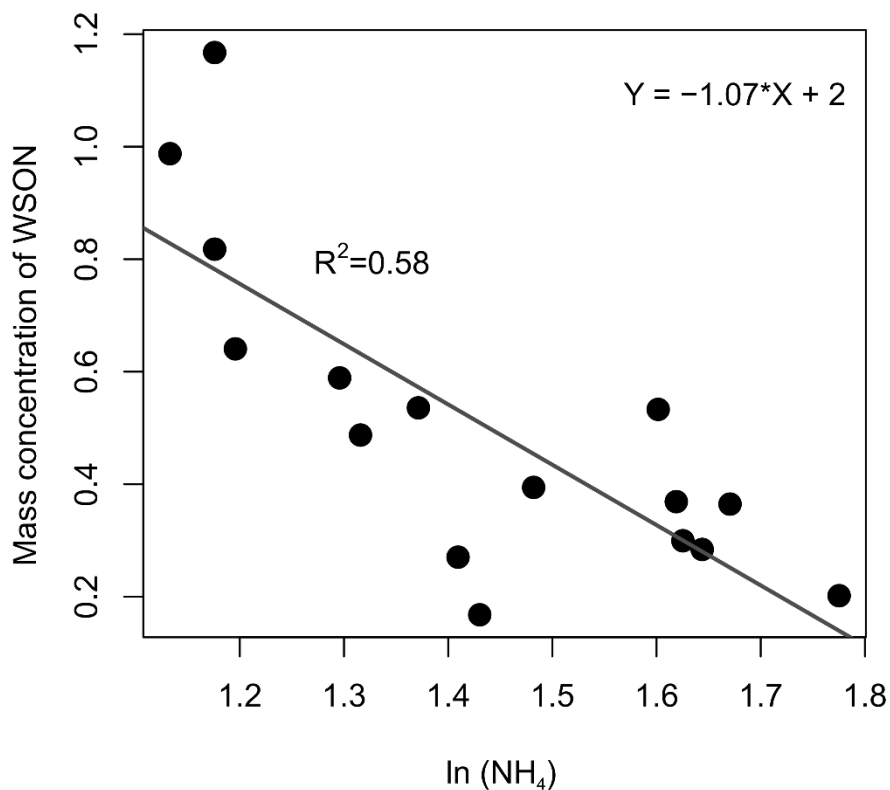


127

128

129 Figure S6. Diurnal variations of RPAs of NOCs, oxidized organics, and ammonium from

130 spring to winter (a-d).

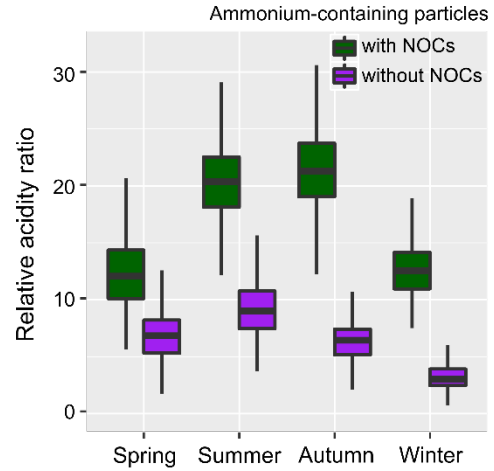
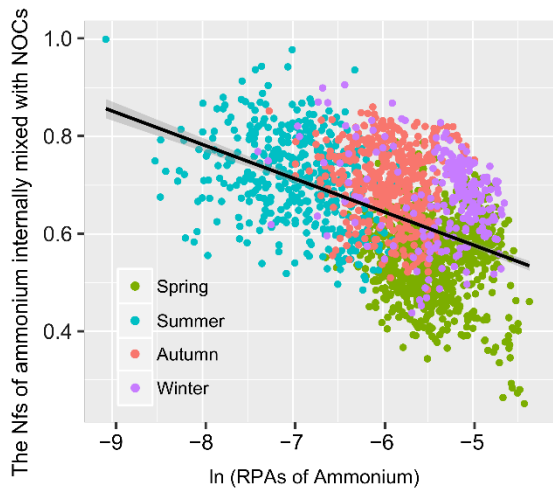


131  
132

133 Figure S7. Relationship between the mass concentration of WSON and ammonium  
 134 (logarithmic transformed) in submicron particles during autumn of 2014. It is noted that  
 135 WSON (represented as the mass concentration of organic N) might not be properly  
 136 regarded as NOCs, as no significant correlation between daily mean mass  
 137 concentrations/fraction of WSON and the RPAs of NOCs. This is probably because the  
 138 daily mean values calculated for the RPAs of NOCs miss the temporal variation  
 139 information. Also, a part of NOCs might not be water-soluble (Cape et al., 2011).

140 During the autumn of 2014, daily size-resolved quartz fiber filter samples were  
 141 collected using an Andersen PM<sub>10</sub> sampler equipped with a size-selective inlet high  
 142 volume cascade impactor (Model SA235, Andersen Instruments Inc.). The filters were  
 143 baked for 4 h in a muffle furnace at 500 °C before use. Water-soluble inorganic ions were

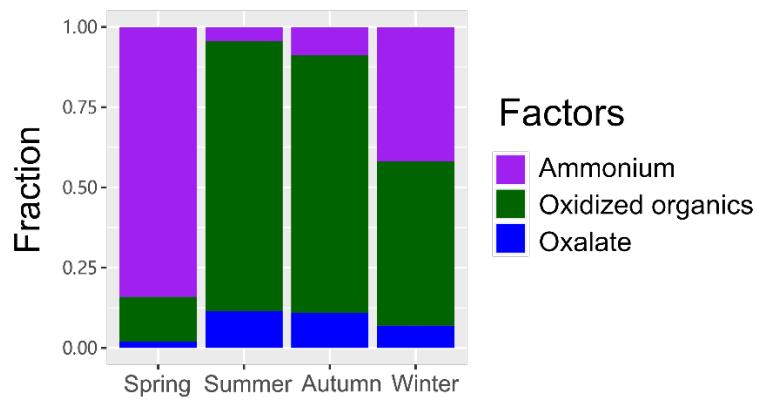
144 analyzed by ion chromatography (Metrohm 883, Switzerland). In addition, water soluble  
145 organic carbon (WSOC) and nitrogen (WSON) were analyzed by a Total Organic Carbon  
146 Analysis Instrument (TOC, Germany). It is noted that NOCs, the oxidized organics, and  
147 ammonium during this period also showed a similar relationship with that during autumn  
148 of 2013.



149  
150

151 Figure S8. Relationship between the Nfs of ammonium that was internally mixed with  
 152 NOCs and RPAs of ammonium (left), and comparison of the relative acidity ratio  
 153 between ammonium-containing particles internally and externally mixed with NOCs  
 154 (right).





155  
156

157 Figure S9. The relative contributions of the PMF-resolved 3-factor to the modelled NOCs  
158 over the seasons.

159 References

- 160 Aiona, P. K., Lee, H. J., Leslie, R., Lin, P., Laskin, A., Laskin, J., and Nizkorodov, S. A.:  
161 Photochemistry of Products of the Aqueous Reaction of Methylglyoxal with Ammonium  
162 Sulfate, *Acs Earth Space Chem.*, 1, 522-532, doi:10.1021/acsearthspacechem.7b00075,  
163 2017.
- 164 Cape, J. N., Cornell, S. E., Jickells, T. D., and Nemitz, E.: Organic nitrogen in the atmosphere —  
165 Where does it come from? A review of sources and methods, *Atmos. Res.*, 102, 30-48,  
166 doi:10.1016/j.atmosres.2011.07.009, 2011.
- 167 Norris, G., Vedantham, R., Wade, K., Zahn, P., Brown, S., Paatero, P., Eberly, S., and Foley, C.  
168 (2009), Guidance document for PMF applications with the Multilinear Engine, edited,  
169 Prepared for the U.S. Environmental Protection Agency, Research Triangle Park, NC.
- 170 Pratt, K. A., Heymsfield, A. J., Twohy, C. H., Murphy, S. M., DeMott, P. J., Hudson, J. G.,  
171 Subramanian, R., Wang, Z. E., Seinfeld, J. H., and Prather, K. A.: In Situ Chemical  
172 Characterization of Aged Biomass-Burning Aerosols Impacting Cold Wave Clouds, *J.*  
173 *Atmos. Sci.*, 67, 2451-2468, doi:10.1175/2010JAS3330.1, 2010.
- 174 Zauscher, M. D., Wang, Y., Moore, M. J. K., Gaston, C. J., and Prather, K. A.: Air Quality Impact  
175 and Physicochemical Aging of Biomass Burning Aerosols during the 2007 San Diego  
176 Wildfires, *Environ. Sci. Technol.*, 47, 7633-7643, doi:10.1021/es4004137, 2013.
- 177 Zhu, S. P., Horne, J. R., Montoya-Aguilera, J., Hinks, M. L., Nizkorodov, S. A., and Dabdub, D.:  
178 Modeling reactive ammonia uptake by secondary organic aerosol in CMAQ: application to  
179 the continental US, *Atmos. Chem. Phys.*, 18, 3641-3657, doi:10.5194/acp-18-3641-2018,  
180 2018.